The 4th Annual IEEE International Conference on
Cyber Technology in Automation, Control and Intelligent Systems
June 4-7, 2014, Hong Kong, China

Towards Stabilizing Parametric Active Contours

Jinchao Liu[1], Zhun Fan[2], Søren Ingvor Olsen[3], Kim Hardam Christensen[4] and Jens Klæstrup Kristensen [5]

***Abstract*— Numerical instability often occurs in evolving of parametric active contours. This is mainly due to the undesired change of parametrization during evolution. In this paper, we propose a new tangential diffusion term to compensate this undesired change. As a result, the parametrization will converge to a parametrization that is proportional to the natural parametrization which implies that the control points of the contour are uniformly distributed. We theoretically prove that this tangential diffusion term is bounded and therefore numerically stable. Several experiments were conducted and verified the feasibility of the proposed tangential diffusion force.**

I. Introduction

One problem that parametric active contours often face is that the control points may bunch together or form self-intersection during evolution. The consequence is that it may lead to unreliable calculation of some quantities such as curvature, normal vector and cause the failure of the evolution. Figure 1 gives an example where parametric active contours failed due to this numerical instability. Numerically, this is due to the irregular spacing of control points, i.e., undesired change of the parametrization which is a side effect of parametric curve evolution. Researchers have been investigating this problem and proposed different techniques to prevent or compensate the undesired change of the parametrization [2], [6], [13], [14], [19].

In terms of the way, discretely or continuously, of solving this problem, these techniques can be classified into two groups. In the first group, the spacing of control points are directly and discretely controlled by re-distributing the control points. For instance in [13], [2], the authors proposed to re-sample the control points every a few iterations or when the distance between neighboring points falls below a predefined threshold. This kind of techniques are straightforward and easy to implement, but also suffer from the limitation that the computation time increases due to the frequent check of the distances. Another group of techniques are proposed in [6], [14], [19], extra tangential forces are introduced to compensate the undesired change of the parametrization during evolution.

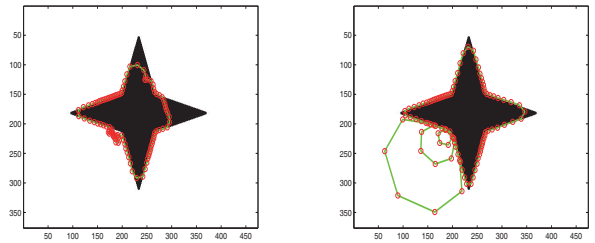

(a) (b)

Fig. 1. An illustration that parametric active contours could be numerical instable during evolution . (a)Iteration 500. Control points bunched together. (b)Iteration 1000. Active contours failed.

In this paper, a new complete tangential diffusion force is presented for redistribution of the control points of a parametric active contour. We will show that by imposing this new complete tangential diffusion force, the change of the parametrization is subject to a diffusion equation. After iterations, the parametrization will converge to one parametrization that is proportional to the natural parametrization, i.e., the uniform distribution of the control points. We will theoretically prove that this tangential diffusion term is bounded and therefore numerically stable. Several experiments is presented and verify the feasibility of the proposed tangential diffusion force.

II. Background and Related Works

A. Active contours: a variational segmentation framework

Active contours, sometimes referred to snakes, were first proposed by Kass etc. in [9]. Since then, much research has been carried out and many extensions and variations have been proposed for numerous applications such as image segmentation and visual tracking[21], [20], [5], [4], [8], [7], [3], [15], [16], [17], [18], [15].

Typically, active contours can be formulated as a minimization of an energy functional. The basic framework introduced by Kass etc. in [9] is as follows. Assume that $\mathscr{C}$ is a parametric curve which is represented as

$$\mathscr{C}(r) = (x(r), y(r)), r \in [0,1] \tag{1}$$

where r is a parametrization of the curve. The energy functional is then defined as follows.

$$E(\mathscr{C}) = \int_0^1 \left(\alpha \| \frac{d\mathscr{C}}{dr} \|^2 + \beta \| \frac{d^2\mathscr{C}}{dr^2} \|^2 + E_{\text{image}} + E_{\text{con}} \right) dr \tag{2}$$

*This work was supported by FORCE Technology and Danish Agency for Science Technology and Innovation

[1]Jinchao Liu was with Department of Management Engineering, Technical University of Denmark. 2800 Kgs. Lyngby, Denmark and was also with Welding and Production Innovation, FORCE Technology. DK-2605 Brødby, Denmark.

[2]Zhun Fan is with College of Engineering, Shantou University. 515063, Shantou, China. zfan@stu.edu.cn

[3] Søren Olsen is with Department of Computer Science, University of Copenhagen. 2100, Copenhagen, Denmark. ingvor@diku.dk

[4] Kim Christensen is with Welding and Production Innovation, FORCE Technology. 2605 Brødby, Denmark. kmc@force.dk

[5] Jens Kristensen was with Welding and Production Innovation, FORCE Technology. 2605 Brødby, Denmark. jens@klaestrup.dk

978-1-4799-3669-4/14/$31.00 © 2014 IEEE

Here $\mathscr{C}$ denotes a curve. The first two terms in the integral are so-called internal forces which characterize the curve itself. By minimizing these two terms, we can regulate or smooth the curve during iteration. The third term is so-called image-dependent term. By minimizing this term, the curve will be driven to the desired boundary of the object. The last term gives rise to extra constraints.

B. Stabilizing Parametric Active Contours

For parametric active contours, the curve is often discretized as a set of control points, i.e. a first-order spline. In practice, it is of great importance to maintain a uniform distribution of the control points along the curve during evolution. It makes the computation of geometric quantities such as the normal vector, curvature easy and stable.

Assume that a 2D continuous active contour $\mathscr{C} = \mathscr{C}(x,y)$ is parameterized by p. In order to have a uniform distribution of the control points, the parametrization p should be proportional to the natural parametrization s, i.e.,

$$g(p) = \|\frac{\partial \mathscr{C}}{\partial p}\| = \zeta \tag{3}$$

where ζ is a constant.

For the initial curve, the control points can be uniformly distributed. However, it has been found that the parametrization may change during evolution. Discretely, the distances between neighboring points may change and are not equal. Assume that the general form of a planar curve evolution can be expressed as follows.

$$\frac{\partial \mathscr{C}(p,t)}{\partial t} = \alpha(p,t)\mathbf{T} + \beta(p,t)\mathbf{N} \tag{4}$$

where $\mathbf{T}$ denotes the tangential vector. $\mathbf{N}$ denotes the outward normal vector. $p \in [0,l]$ is a parametrization. t is the artificial evolving time. In [10], the author proved that $g(p,t)$ evolves according to the following equation:

$$\frac{\partial g(p,t)}{\partial t} = \frac{\partial \alpha}{\partial p} + \beta \kappa g \tag{5}$$

where κ denotes the curvature.

It is worth noting that the tangential term α does not affect the shape of the curve but change the parametrization. The normal term β is, on the other hand, responsible for the change of the shape. Without considering the problem of numerical instability, in fact only β is essential for the curve evolution. This is the reason why only the normal term β is considered in the level set methods since one does not parameterize the curve in the level set methods. But in the parametric active contours methods, α becomes important and it is possible to actively control the evolution of the parametrization by imposing an additional tangential term.

In [6], the authors proposed a tangential force to control the metric function $g(p,t)$.

$$f_{\text{tangent}} = (\frac{\partial^2 \mathscr{C}}{\partial p^2} \cdot \mathbf{T})\mathbf{T} = \frac{\partial g}{\partial p}\mathbf{T} \tag{6}$$

By imposing this tangential force, $g(p,t)$ is governed by the following partial differential equation:

$$\frac{\partial g}{\partial t} = \frac{\partial^2 g}{\partial p^2} + \beta \kappa g \tag{7}$$

The above equation corresponds to the diffusion of $g(p,t)$ along the curve if β is small enough. The authors argued that when the steady state is reached, the parametrization will be proportional to the natural parametrization. However, the assumption that β is small enough is often not true in practice. The additional tangential force is insufficient to compensate all the undesired change of parametrization and therefore incomplete. The evolution of parametrization does not follow the exact heat diffusion equation. Inspired by this work, we proposed a complete tangential force that can offset all the undesired change of the parametrization.

III. A Complete Tangential Diffusion Force

It has been discussed that an additional tangential force $\alpha(p,t)$ can be introduced to regulate the evolution of the parametrization. Note that if α is defined as follows:

$$\frac{\partial \alpha}{\partial p} = c^2 \frac{\partial^2 g}{\partial p^2} - \beta \kappa g \tag{8}$$

where c is a constant. Substituting Equation (8) into Equation (5) leads to

$$\frac{\partial g}{\partial t} = c^2 \frac{\partial^2 g}{\partial p^2} \tag{9}$$

This is a *heat equation* with the periodic boundary condition $g(0,t) = g(l,t)$ and initial value $g(p,0)$. The solution is given as follow [1].

$$g(p,t) = a_0 + \sum_{n=1}^{\infty} [a_n cos(\frac{n\pi}{l}p) + b_n \sin(\frac{n\pi}{l}p)]e^{-(\frac{cn\pi}{l})^2 t} \tag{10}$$

where

$$a_0 = \frac{1}{l}\int_0^l g(p,0)dp \tag{11}$$

$$a_n = \frac{2}{l}\int_0^l \cos(\frac{n\pi}{l}p)g(p,0)dp \tag{12}$$

$$b_n = \frac{2}{l}\int_0^l \sin(\frac{n\pi}{l}p)g(p,0)dp \tag{13}$$

Let $t \to \infty$, we obtain the steady state solution $g(p,\infty) = a_0$. Note that

$$a_0 = \frac{1}{l}\int_0^l g(p,0)dp = \frac{1}{l}\int_{\mathscr{C}_0} ds = \frac{\text{length}(\mathscr{C}_0)}{l} \tag{14}$$

Where $\mathscr{C}_t, t \in [0,\infty)$ denotes the curve at the time t. Very often l is set to 1, then $g(p,\infty) = \text{length}(\mathscr{C}_0)$. This proves that after sufficient iterations, the parametrization will be proportional to the natural parametrization. In other words, the control points will be distributed uniformly.

The tangential force proposed here is superior to the one in [6] because theoretically it can offset the undesired change of the parametrization completely and therefore control the parametrization more precisely. In the following, we shall prove this both analytically and experimentally.

A. Boundedness of Tangential Evolution

In this section we shall prove that the proposed tangential redistribution force $\alpha(p,t)$ is bounded i.e., $\sup_{p,t}\{\|\alpha(p,t)\|\} < \infty$ for every $p \in [0,l], t \in [t_0,\infty)$ and therefore numerically stable.

Integrating both sides of Equation (8) along the curve yields

$$\alpha(p,t) = \int_0^p (c^2 \frac{\partial^2 g(p,t)}{\partial p^2} + \beta(p,t)\kappa(p,t)g(p,t))dp \quad (15)$$

Hence,

$$\|\alpha(p,t)\| = \|\int_0^p (c^2 \frac{\partial^2 g(p,t)}{\partial p^2} + \beta(p,t)\kappa(p,t)g(p,t))dp\| \quad (16)$$

$$\leq \int_0^l \|c^2 \frac{\partial^2 g(p,t)}{\partial p^2} + \beta(p,t)\kappa(p,t)g(p,t)\|dp \quad (17)$$

$$\leq \int_0^l \|c^2 \frac{\partial^2 g(p,t)}{\partial p^2}\|dp + \int_0^l \|\beta(p,t)\kappa(p,t)g(p,t)\|dp \quad (18)$$

$$= \int_0^l \|\frac{\partial g(p,t)}{\partial t}\|dp + \int_0^l \|\beta(p,t)\kappa(p,t)g(p,t)\|dp \quad (19)$$

Taking the partial derivative of both sides of Equation (10) with respect to t yields

$$\frac{\partial g(p,t)}{\partial t} = \sum_{n=1}^{\infty} -(\frac{cn\pi}{l})^2 [a_n \cos(\frac{n\pi}{l}p) + b_n \sin(\frac{n\pi}{l}p)]e^{-(\frac{cn\pi}{l})^2 t} \quad (20)$$

Substituting Equation (20) into the first term of Equation (19), we have

$$\int_0^l \|\frac{\partial g(p,t)}{\partial t}\|dp \quad (21)$$

$$= \int_0^l \|\sum_{n=1}^{\infty} -(\frac{cn\pi}{l})^2 [a_n \cos(\frac{n\pi}{l}p) + b_n \sin(\frac{n\pi}{l}p)]e^{-(\frac{cn\pi}{l})^2 t}\|dp \quad (22)$$

$$\leq \int_0^l \sum_{n=1}^{\infty} \|(\frac{cn\pi}{l})^2 [a_n \cos(\frac{n\pi}{l}p) + b_n \sin(\frac{n\pi}{l}p)]e^{-(\frac{cn\pi}{l})^2 t}\|dp \quad (23)$$

$$\leq M \int_0^l \sum_{n=1}^{\infty} (\frac{cn\pi}{l})^2 e^{-(\frac{cn\pi}{l})^2 t} dp \quad (24)$$

$$= Ml \sum_{n=1}^{\infty} \lambda_n^2 e^{-\lambda_n^2 t} \quad (25)$$

where $\lambda_n = \frac{cn\pi}{l}$ and $M = \sup_{p\in[0,l]}\{\|a_n \cos(\frac{n\pi}{l}p) + b_n \sin(\frac{n\pi}{l}p)\|\}$. Now we shall prove that the series of functions $\sum_{n=1}^{\infty} \lambda_n^2 e^{-\lambda_n^2 t}$ converges. In fact, using *DÁlembertś ratio test*, it can be proved that the series $\sum_{n=1}^{\infty} \lambda_n^2 e^{-\lambda_n^2 t_0}$ is convergent, hence $\sum_{n=1}^{\infty} \lambda_n^2 e^{-\lambda_n^2 t}$ converges, i.e.,

$$\sum_{n=1}^{\infty} \lambda_n^2 e^{-\lambda_n^2 t} \leq \sum_{n=1}^{\infty} \lambda_n^2 e^{-\lambda_n^2 t_0} \leq W_1 \quad (26)$$

where W_1 is the upper bound. Therefore, the first integral of Equation (19) is bounded by MlW_1.

Now let us examine the second integral of Equation (19). First, assume that $\beta(p,t)\kappa(p,t)$, which is normally defined by the need of deforming the curve so as to attach it to the desired object boundary, is bounded by F.

$$\int_0^l \|\beta(p,t)\kappa(p,t)g(p,t)\|dp \leq F \int_0^l \|g(p,t)\|dp \quad (27)$$

$$= F \int_0^l \|a_0 + \sum_{n=1}^{\infty} [a_n \cos(\frac{n\pi}{l}p) + b_n \sin(\frac{n\pi}{l}p)]e^{-(\frac{cn\pi}{l})^2 t}\|dp \quad (28)$$

$$\leq Fl|a_0| + \sum_{n=1}^{\infty} \int_0^l \|[a_n \cos(\frac{n\pi}{l}p) + b_n \sin(\frac{n\pi}{l}p)]e^{-(\frac{cn\pi}{l})^2 t}\|dp \quad (29)$$

$$\leq Fl|a_0| + Ml \sum_{n=1}^{\infty} e^{-(\frac{cn\pi}{l})^2 t} \quad (30)$$

Similarly we can prove that $\sum_{n=1}^{\infty} e^{-(\frac{cn\pi}{l})^2 t}$ converges and bounded by W_2. Combining these two terms, it is evident to see that α is bounded, i.e.,

$$\sup_{p\in[0,l],t\in[t_0,\infty)} \left\{\|\alpha(p,t)\|\right\} \leq Ml(W_1 + W_2) + Fl|a_0| < \infty \quad (31)$$

B. Convergence Speed of Tangential Diffusion

Recall that Equation (10) gives the behavior of the parametrization $g(p,t)$ after adding an tangential regulating force $\alpha(p,t)$. It has been proved that $g(p,t)$ will converge to the parametrization that is proportional to the natural parametrization which indicates that the control points will be uniformly distributed. We also prove that $\alpha(p,t)$ is bounded. In practice, another important issue is to investigate the convergence speed of the proposed tangential diffusion. Again Equation (10) shows that it exponentially converges to the steady-state solution and the order is given by $(\frac{cn\pi}{l})^2$. Theoretically, increasing c will speed up the convergence of the tangential diffusion. However, c can not be selected arbitrarily for the reason of numerical stability of tangential diffusion.

C. Numerical Implementation

The proposed additional tangential diffusion force α is defined as shown in Equation (8). In practice, we discretize it by means of finite difference method.

$$\frac{\alpha_{i+1} - \alpha_i}{\Delta p} = c^2 \frac{g_{i+1} - 2g_i + g_{i-1}}{(\Delta p)^2} - \beta_i \kappa_i g_i \quad (32)$$

Reordering the terms gives us

$$\alpha_{i+1} = \alpha_i + \frac{c^2}{\Delta p}(g_{i+1} - 2g_i + g_{i-1}) - \Delta p \beta_i \kappa_i g_i \quad (33)$$

where

$$g_i = \|\frac{\mathscr{C}_{i+1} - \mathscr{C}_i}{\Delta p}\| \quad (34)$$

IV. Experiments

To validate the proposed complete tangential diffusion term, two experiments have been conducted.

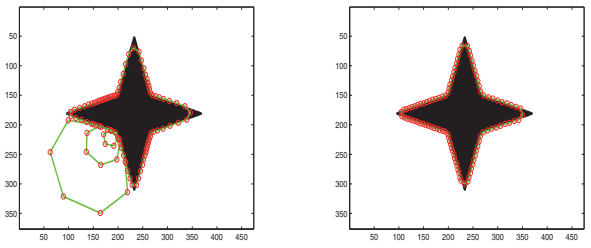

(a) (b)

Fig. 2. A comparison of curve evolution with or without the proposed tangential force in a synthetic image. (a)Without tangential forces. (b)With the proposed tangential force.

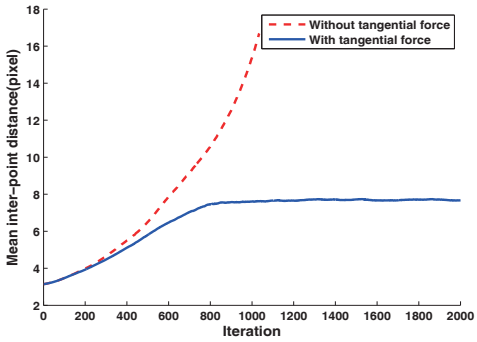

(a)

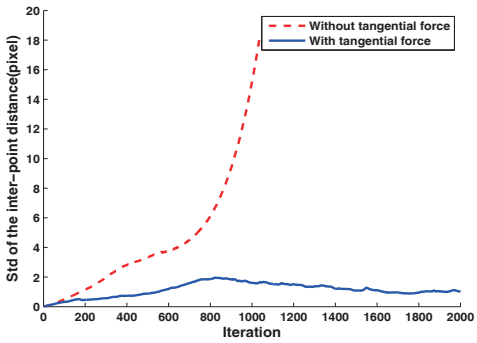

(b)

Fig. 3. A comparison of curve evolution with or without the proposed tangential force in a synthetic image. (a) Mean of the inter-point distance. (b) Standard deviation of the inter-point distance.

A. Image segmentation

Firstly, we tested the proposed term on the synthetic image which is also shown in Fig. 1. The result can be seen in Fig. 2. In Fig. 2(a), the numerical instability occurred when without using any tangential force and several loops were formed and eventually failed to segment the star. On the other hand, with the proposed tangential diffusion term, it succeeded in evolving stably and capturing the boundary of the star, as shown in Fig. 2(b). Fig. 3 shows the mean and standard deviation of the distance between the neighboring points.

B. A real-world application: weld pool boundary tracking

In modern industry, arc welding plays an important role for jointing materials. It however still heavily relies on the human welders. To automate the arc welding process, extracting visual information is of great importance. Many researchers and engineers have been developing different kinds of vision system to obtain visual information of the seam and the weld pool. A more detailed introduction can be found in [12].

To tackle this problem, we proposed a Feature Selected Adaboost Geodesic Active Region (FSA-GAR). The Euler - Lagrange equation is defined as followed.

$$\frac{\partial \mathbf{x}(t)}{\partial t} = \eta_1 \underbrace{g(p_b(\mathbf{x}))\kappa\vec{\mathbf{n}}}_{\text{geodesic internal force}} - \eta_2 \underbrace{(\nabla g(p_b(\mathbf{x}))\cdot\vec{\mathbf{n}})\vec{\mathbf{n}}}_{\text{boundary-based force}} - \underbrace{\gamma \log \frac{p_{\text{in}}(I(\mathbf{x}))}{p_{\text{out}}(I(\mathbf{x}))}\vec{\mathbf{n}}}_{\text{region-based force}} \tag{35}$$

The active contours used in experiment 1 and 2 are active contours driven by region-based forces. For the weld pool image, we use the proposed Feature Selective Adaboosting Geodesic Active Region(FSA-GAR). The results are presented and discussed here.

Figure 2 shows the results in a synthetic image. In Figure 2(a), the numerical instability occurred when without using any tangential force and several loops were formed and eventually failed to segment the star. On the other hand, with the proposed tangential diffusion term, it succeeded in evolving stably and capturing the boundary of the star, as shown in Figure 2(b). Figure 2(c) and (d) show the mean and standard deviation of the distance between the neighboring points.

Fig. 5 and 6 show another two examples in an image of a plane and a typical weld pool image. The results confirm again that the proposed tangential diffusion term can stabilize the evolution of parametric active contours.

The comparison between the complete tangential force proposed here and the incomplete one proposed in [6] has also been carried out. The results are presented in Fig. 7. It can be seen that with the complete tangential force, the control points are much more evenly distributed.

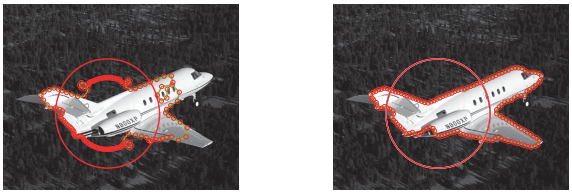

(a) (b)

Fig. 4. A comparison of curve evolution with or without the proposed tangential force in an image of a plane. The red circles indicate the initial contours. The final curve are marked in green. (a)Without tangential force. (b)With tangential force.

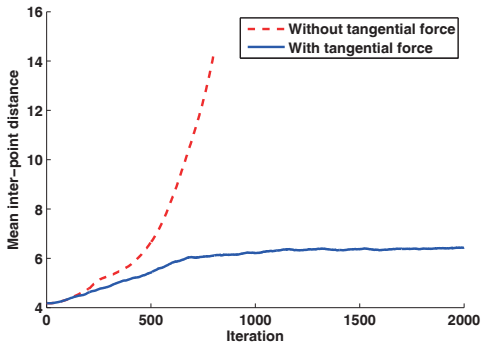

(a) Mean of the inter-point distance.

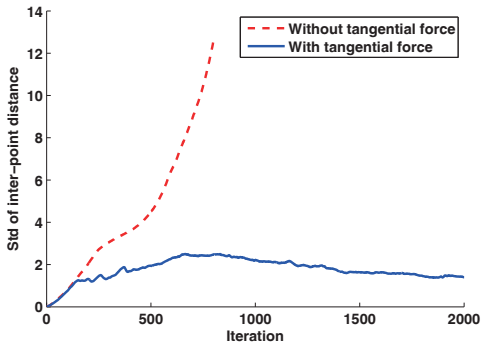

(b) Standard deviation of the inter-point distance.

Fig. 5. A comparison of curve evolution with or without the proposed tangential force in an image of a plane. The red circles indicate the initial contours. The final curve are marked in green.

V. Conclusions

Parametric active contours often face the problem of numerical instability during evolution which is mainly caused by undesired change of the parametrization. In this paper, a new tangential diffusion term is proposed to compensate this undesired change. We analytically prove that by adding this term, the parametrization will converge to the one that is proportional to the natural parametrization. This implies that the control points are distributed uniformly. The experiments in synthetic and real-world images verify the feasibility of the proposed tangential diffusion term.

References

[1] Asmar, N. H. *Partial Differential Equations with Fourier Series and Boundary Value Problems*, 2nd ed. Prentice Hall, May 2004.

[2] Cham, T.-J., and Cipolla, R. Automated b-spline curve representation incorporating mdl and error-minimizing control point insertion strategies. *Pattern Analysis and Machine Intelligence, IEEE Transactions on 21*, 1 (Jan 1999), 49 –53.

[3] Chan, T., Esedoglu, S., and Ni, K. Histogram based segmentation using wasserstein distances. In *Scale Space and Variational Methods in Computer Vision*, F. Sgallari, A. Murli, and N. Paragios, Eds., vol. 4485 of *Lecture Notes in Computer Science*. Springer Berlin / Heidelberg, 2007, pp. 697–708.

[4] Chan, T., and Shen, J. *Image Processing And Analysis: Variational, PDE, Wavelet, And Stochastic Methods*. Society for Industrial and Applied Mathematic, September 2005.

[5] Chan, T., and Vese, L. Active contours without edges. *Image Processing, IEEE Transactions on 10*, 2 (Feb 2001), 266 –277.

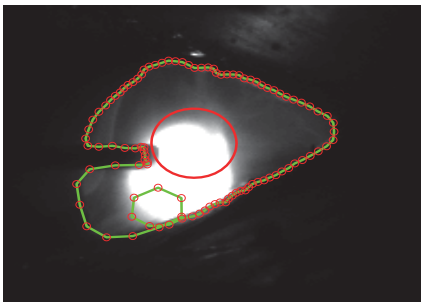

(a) without tangential force.

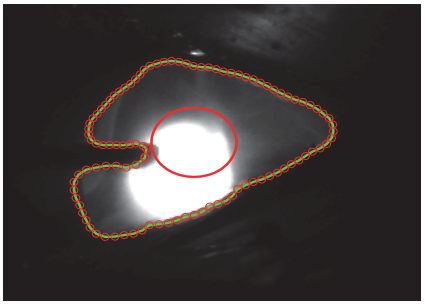

(b) with tangential force.

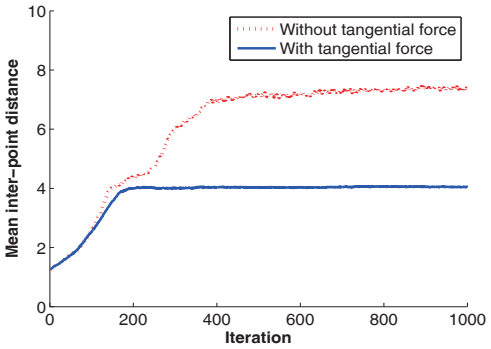

(c) Mean of the inter-point distance.

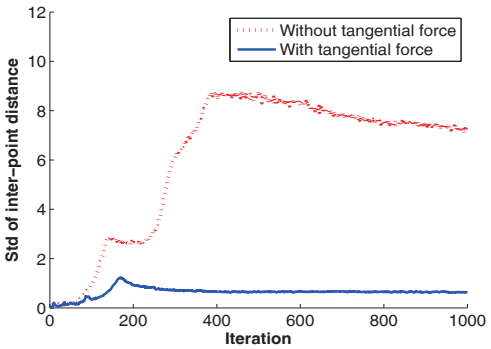

(d) Standard deviation of the inter-point distance.

Fig. 6. A comparison of curve evolution with or without the proposed tangential force in a weld pool image. The red circles indicate the initial contours. The final curve are marked in green.

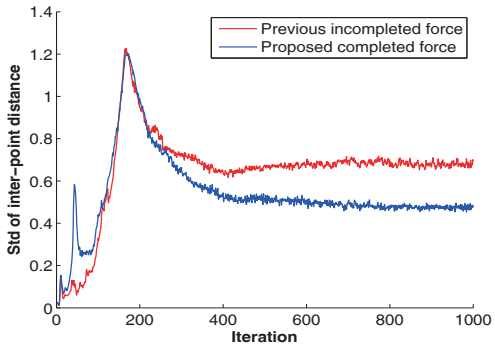

Fig. 7. A comparison of the proposed complete tangential force and the previous incomplete tangential force in the weld pool image. The x-axis represents the iteration. The y-axis represents the standard deviation of the distance between neighboring points.

[6] DELINGETTE, H., AND MONTAGNAT, J. Shape and topology constraints on parametric active contours. *Computer Vision and Image Understanding 83* (Aug 2001), 140–171.

[7] FRITSCHER, K., GRUNERBL, A., AND SCHUBERT, R. 3d image segmentation using combined shape-intensity prior models. *International Journal of Computer Assisted Radiology and Surgery 1* (2007), 341–350.

[8] HERBULOT, A., JEHAN-BESSON, S., BARLAUD, M., AND AUBERT, G. Shape gradient for image segmentation using information theory. In *Acoustics, Speech, and Signal Processing, 2004. Proceedings. (ICASSP '04). IEEE International Conference on* (may 2004), vol. 3, pp. iii – 21–4 vol.3.

[9] KASS, M., WITKIN, A., AND TERZOPOULOS, D. Snakes: Active contour models. *International Journal of Computer Vision 1*, 4 (1988), 321–331.

[10] KIMIA, B. B., TANNENBAUM, A., AND ZUCKER, S. W. On the evolution of curves via a function of curvature. i. the classical case. *Journal of Mathematical Analysis and Applications 163*, 2 (1992), 438 – 458.

[11] LIU, J., AND FAN, Z. *Passive Visual Sensing in Automatic Arc Welding*. PhD thesis, Technical University of Denmark (DTU), Kgs. Lyngby, Denmark, 2011.

[12] LIU, J., FAN, Z., OLSEN, S., CHRISTENSEN, K., AND KRISTENSEN, J. Weld pool visual sensing without external illumination. In *Automation Science and Engineering (CASE), 2011 IEEE Conference on* (2011), pp. 145–150.

[13] MENET, S., SAINT-MARC, P., AND MEDIONI, G. Active contour models: overview, implementation and applications. In *Systems, Man and Cybernetics, 1990. Conference Proceedings., IEEE International Conference on* (Nov 1990), pp. 194 –199.

[14] MIKULA, K., AND SEVCOVIC, D. Computational and qualitative aspects of evolution of curves driven by curvature and external force. *Computing and Visualization in Science 6* (2004), 211–225.

[15] OLIVIER, J., BONE, R., ROUSSELLE, J.-J., AND CARDOT, H. Active contours driven by supervised binary classifiers for texture segmentation. In *Advances in Visual Computing* (2008), vol. 5358 of *Lecture Notes in Computer Science*, Springer Berlin / Heidelberg, pp. 288–297.

[16] PARAGIOS, N., AND DERICHE, R. Geodesic active regions: A new framework to deal with frame partition problems in computer vision. *Journal of Visual Communication and Image Representation 13*, 1-2 (2002), 249 – 268.

[17] PARAGIOS, N., AND DERICHE, R. Geodesic active regions and level set methods for supervised texture segmentation. *Int. J. Comput. Vision 46* (February 2002), 223–247.

[18] PARAGIOS, N., AND DERICHE, R. Geodesic active regions and level set methods for motion estimation and tracking. *Computer Vision and Image Understanding 97*, 3 (2005), 259 – 282.

[19] SRIKRISHNAN, V., AND CHAUDHURI, S. Stabilization of parametric active contours using a tangential redistribution term. *Image Processing, IEEE Transactions on 18*, 8 (Aug. 2009), 1859 –1872.

[20] XU, C., AND PRINCE, J. Snakes, shapes, and gradient vector flow. *Image Processing, IEEE Transactions on 7*, 3 (Mar 1998), 359 –369.

[21] XU, C., AND PRINCE, J. L. Medical image segmentation using deformable models. *Handbook of Medical Imaging – Volume 2: Medical Image Processing and Analysis 2* (2000), 129–174.